KARYA ILHAM PUBLISHING
CONNECTING MINDS, BRIDGING IDEAS, INSPIRING READERS

Future Energy and Environment Letters

Journal homepage:
https://karyailham.com.my/index.php/feel
ISSN: 3083-8940

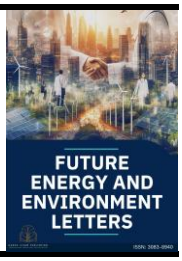

A Review of Bifacial Perovskite Solar Cells

Shafidah Shafian[1,*]

[1] Solar Energy Research Institute, Universiti Kebangsaan Malaysia, 43600 Bangi, Selangor, Malaysia

ARTICLE INFO

Article history:
Received 18 April 2025
Received in revised form 12 June 2025
Accepted 20 June 2025
Available online 30 June 2025

Keywords:
Bifacial; transparent; perovskite; solar cell; photovoltaic

ABSTRACT

Bifacial perovskite solar cells (B-PSCs) have emerged as a promising solution to enhance photovoltaic efficiency by harvesting light from both front and rear surfaces. While perovskite materials offer high power conversion efficiency and low-cost fabrication, traditional single-sided architectures limit their energy-harvesting potential. The purpose of this research is to systematically analyze recent progress in materials design, device architecture, and optical management strategies for B-PSCs. Key results indicate that optimized electrodes and interlayers significantly improve rear-side transparency, responsivity and overall energy yield. B-PSCs represent a viable pathway toward next-generation, high-efficiency photovoltaics, though further work is needed to address stability, large-scale production, and long-term operational performance.

1. Introduction

The growing demand for renewable energy solutions has catalyzed significant advancements in photovoltaic technologies, with perovskite solar cells (PSCs) emerging as one of the most promising alternatives to traditional silicon-based systems due to their remarkable power conversion efficiencies (PCEs), low-cost fabrication processes, and material versatility [1]. Among the various device architecture in this field, bifacial perovskite solar cells (B-PSCs) have gained considerable attention due to their ability to harvest light from both front and rear surfaces, effectively enhancing total energy generation [2].

The core theoretical advantage of B-PSCs lies in their ability to exploit direct, diffuse, and ground-reflected light, phenomena explained by radiative transfer theory and the albedo effect, as illustrated in Figure 1. The latter refers to the fraction of solar radiation reflected from the ground or nearby surfaces and captured through the rear side of the solar cell. This dual-side illumination enables higher photocurrent generation compared to traditional monofacial architectures, thus expanding their operational efficiency in real-world environments such as building-integrated photovoltaics (BIPVs) [3], floating solar systems [4], and agrivoltaics installations [5].

In addition to outdoor applications, recent research has underscored the remarkable performance of B-PSCs under indoor lighting conditions. The high absorption coefficient, tunable

* *Corresponding author.*
E-mail address: norshafidah@ukm.edu.my

https://doi.org/10.37934/feel.3.1.3649

bandgap, and low-light response of perovskite materials make them highly suitable for energy harvesting in artificial or low-intensity environments. This opens new possibilities for B-PSCs in powering indoor Internet-of-Things (IoT) devices and self-powered electronics [6,7]. Notable studies have demonstrated promising PCE under indoor LED illumination, reinforcing the versatility of B-PSCs for multifunctional energy solutions [8,9]

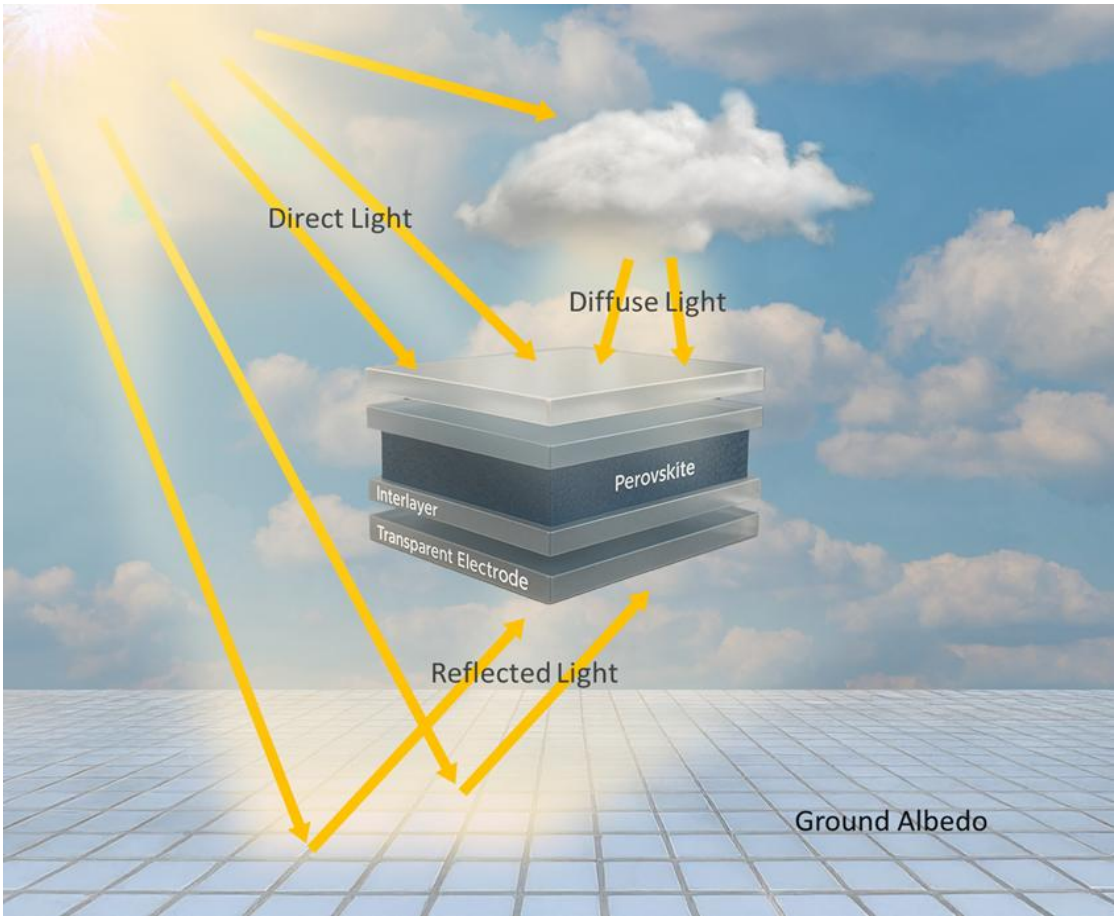

Fig. 1. Schematic illustration of a bifacial perovskite solar cell receiving light from both the front and rear sides, including direct sunlight, diffuse sky radiation, and ground-reflected light due to the albedo effect

B-PSCs exploit the unique optoelectronic properties of perovskite materials, which contribute to their high efficiency and versatility. One of the most notable features is their high absorption coefficient, which allows them to capture a larger portion of the solar spectrum, enhancing their PCE. In addition, B-PSCs demonstrate exceptional defect tolerance, meaning they are less affected by imperfections in the material, ensuring stable performance over time. They also possess long carrier lifetimes and extended carrier diffusion lengths, which enable charge carriers to travel further without recombining, ultimately improving efficiency. The low surface recombination in B-PSCs minimizes energy losses at the interfaces, while passivated interfaces help reduce defects and increase the overall device stability. Furthermore, the tunable band alignment of B-PSCs allows for optimization of the energy levels, making them adaptable to a range of light conditions and improving their overall performance.

B-PSCs also demand advanced structural engineering to achieve effective charge separation under dual-illumination. This typically involves a symmetrical or semi-transparent stack comprising transparent conductive oxides, passivated charge transport layers, and optimized band alignment to

facilitate charge collection from both surfaces [10,11]. Moreover, B-PSCs are made from abundant and cost-effective materials, and their improved efficiency reduces the need for excessive material use, resulting in lower production and operational costs. This combination of higher energy output, increased efficiency, durability, and economic advantages positions B-PSCs as a compelling alternative to traditional monofacial cells in the rapidly expanding solar energy market.

This review provides a comprehensive overview of B-PSCs, exploring their structure, performance, and the underlying mechanisms that influence their efficiency. Despite these promising attributes, the development of B-PSCs faces several challenges, including issues related to material stability, carrier recombination, and the overall efficiency. By delving into the latest research and technological advancements, we aim to highlight the potential of B-PSCs as a transformative technology in the pursuit of more efficient and cost-effective solar energy solutions.

2. Working Principle of B-PSCs

2.1 Light Absorption, Charge Generation and Transport

B-PSCs operate by harnessing incident light from both the front and rear surfaces of the device, thereby extending their photoconversion potential beyond that of conventional monofacial designs. The core of the device comprises a organic-inorganic hybrid perovskite such as methylammonium lead iodide, $MAPbI_3$ ($CH_3NH_3PbI_3$) and formamidinium lead iodide, $FAPbI_3$ ($CH(NH_2)2PbI_3$), or all-inorganic perovskite such as caesium lead iodide ($CsPbI_3$) or its multi-cation variants which serves as the light-absorbing material due to its direct bandgap (typically ~1.5–1.8 eV) and exceptionally high absorption coefficients (>10^5 cm^{-1}) [12-15].

Upon photon absorption, electron-hole pairs are generated and rapidly dissociate into free carriers due to the low exciton binding energy (~10–50 meV) intrinsic to perovskite materials. The efficient separation and collection of these carriers rely on a carefully engineered heterojunction stack. Electrons are typically transported through an electron transport layer (ETL) such as titanium dioxide (TiO_2), tin dioxide (SnO_2), or zinc oxide (ZnO) while holes migrate through a hole transport layer (HTL), often composed of Spiro-OMeTAD, Poly[bis(4-phenyl)(2,4,6-trimethylphenyl)amine] (PTAA), or nickel oxide (NiO_X) [13, 16-18]. The energy level alignment between the perovskite and transport layers is critical for minimizing potential barriers and recombination losses.

In bifacial architectures, both electrodes must be at least partially transparent to facilitate dual-side illumination. Transparent conductive oxides (TCOs) such as indium tin oxide (ITO) or fluorine-doped tin oxide (FTO) are typically employed at one or both interfaces. Charge collection is further influenced by the diffusion length and carrier mobility in the perovskite film, as well as the conductivity of the electrode. Additionally, bifacial designs often incorporate optical enhancement strategies such as photonic structures to maximize light trapping and internal photon recycling, thus enhancing charge generation without compromising extraction efficiency.

2.2 Performance Metrics in B-PSCs

The evaluation of B-PSCs extends beyond the conventional efficiency metrics used for monofacial solar cells due to their unique dual-illumination capability. While PCE remains a foundational metric, a more comprehensive performance characterization must account for additional parameters that reflect dual-sided light harvesting. These include the bifacial factor (BF), which quantifies the ratio of rear-side to front-side efficiency; the bifacial gain (BG), which measures the net improvement in power output compared to monofacial devices; and the energy yield (kWh/kWp/day), which captures long-term power generation under real-world conditions.

2.2.1 Power conversion efficiency (PCE)

PCE is calculated using the standard formula following Eq. (1):

$$PCE = \frac{Jsc \times Voc \times FF}{Pin} \quad (1)$$

where, J_{SC} is short-circuit current density, V_{OC} is open-circuit voltage, FF is fill factor and Pin is the incident power density typically 100 mW/cm^2 if measured under AM1.5G 1 sun illumination. In B-PSCs, this value is typically determined separately for the front and rear surfaces due to varying optical paths and incident angles.

2.2.2 Bifacial factor (BF)

To capture the performance symmetry of bifacial devices, the BF is defined as shown in Eq. (2):

$$BF\ (\%) = \frac{PCE_{rear}}{PCE_{front}} \times 100 \quad (2)$$

BF provides a dimensionless indication of rear-side utilization efficiency. High BF values (typically above 85%) are indicative of well-optimized rear electrode designs with minimal optical and electrical losses.

2.2.3 Bifacial gain (BG)

BG quantifies the net improvement in power output when both sides are utilized compared to a standard monofacial cell. BG is expressed as the percentage increase in energy yield attributable to rear-side illumination under standard testing conditions. This metric is particularly important for real-world evaluations where diffuse and ground-reflected light (characterized through the albedo effect) can significantly enhance overall energy production as shown by Eq. (3):

$$BG\ (\%) = \frac{P_{bifacial} - P_{monofacial}}{P_{monofacial}} \times 100 \quad (3)$$

where $P_{bifacial}$ is the power output or energy yield from the bifacial solar cell (front and rear) and $P_{monofacial}$ is the power output or energy yield from a monofacial solar cell (front only).

2.2.4 Energy yield

Energy yield typically expressed in kWh/kWp/day or kWh/kWp/year serves as a pivotal performance indicator for B-PSCs. This metric encapsulates the cumulative electrical output over extended temporal scales, inherently accounting for diurnal and seasonal variations in solar irradiance, temperature, and environmental conditions. Notably, energy yield reflects the tangible benefits of dual-sided light collection, especially in deployment scenarios where ground-reflected irradiance (albedo) significantly enhances rear-side illumination. As such, elevated energy yields in B-PSCs substantiate their potential for high-efficiency deployment in real-world applications.

3. Performance of B-PSCs

Over the past decade, B-PSCs have demonstrated rapid progress in efficiency and architecture refinement. Table 1 shows the recent progress in B-PSCs technology for 10 years starting from 2015 to 2025.

Table 1
Summary of bifacial PSCs with PCE from front and rear side with bifacial factor

Author/ Year	Device Structure	PCE (%)		BF
		Front	Rear	(%)
Fu *et al.,* [19]	FTO/ZnO/PCBM/$CH_3NH_3PbI_3$/MoO_3/In_2O_3:H	14.2	9.6	67.60
Xiao *et al.,* [20]	ITO/bl-TiO_2/m-TiO_2/ $CH_3NH_3PbI_3$/FTO	8.67	8.27	95.38
	ITO/bl-TiO_2/m-TiO_2/ $CH_3NH_3PbI_3$/PEDOT/FTO	12.33	11.88	96.35
Pang *et al.,* [21]	ITO/PEDOT:PSS/ $CH_3NH_3PbI_3$/PCBM/Ag	8.04	5.24	65.11
	ITO/PEDOT:PSS/ $CH_3NH_3PbI_3$/PCBM/Ag/MoO_X	10.40	6.54	62.88
	ITO/PEDOT:PSS/ $CH_3NH_3PbI_3$/PCBM/PEIE/Ag/MoO_X	13.55	8.41	62.06
	ITO/PEDOT:PSS/$CH_3NH_3PbI_3$/PCBM/PEIE/Ag/MoO_X/back reflector	14.5	11.37	78.41
Hanmandlu *et al.,* [22]	ITO/PEDOT:PSS/ $CH_3NH_3PbI_3$/BCP/Ag/MoO_3	13.49	9.61	71.23
Fan *et al.,* [23]	FTO/TiO_2/$FA_{0.5}MA_{0.5}PbI_{3-x}Cl_X$ /CuSCN/Au	12.47	8.74	70.09
Martinez-D. *et al.,* [24]	ITO/SnO_2/TiO_2/ $CH_3NH_3PbI_3$/PTAA/Au	12.9	9.1	70.54
Deluca *et al.,* [25]	FTO/TiO_2/$Cs_{0.05}FA_{0.79}MA_{0.16}PbI_{2.49}Br_{0.51}$/CuSCN/ITO	1.7	1.4	82.35
Pang *et al.,* [26]	ITO/PEDOT:PSS/$Cs_{0.05}$ $FA_{0.3}$ $MA_{0.7}$ $PbI_{2.51}Br_{0.54}$/PCBM/BCP/ Ag/V_2O_5	14.01	8.91	63.60
	ITO/PEDOT:PSS/ $Cs_{0.05}$ $FA_{0.3}$ $MA_{0.7}$ $PbI_{2.51}Br_{0.54}$/PCBM/BCP/ Ag/V_2O_5/reflector	15.39	12.44	80.83
Li *et al.,* [27]	FTO/c-TiO_2/m-TiO_2/CsPbBr$_3$/carbon/CsPbBr$_3$/m-TiO_2/c-TiO_2/FTO	7.55	7.44	98.54
Lee *et al.,* [28]	FTO/c-TiO_2/m-TiO_2/ $CH_3NH_3PbI_3$/CT/MoO_X/ITO	14.96	13.61	90.98
Chiang *et al.,* [29]	FTO/TiO_x/mp TiO_2/ $CH_3NH_3PbI_3$/Spiro/MoO_X/IZO	16.40	15.26	93.04
Chen *et al.,* [30]	ITO/NiO_X/$FA_{0.3}MA_{0.7}PbI_{3-x}Cl_x$/$PC_{61}BM$/BCP/Ag	12.7	7.33	57.72
	ITO/NiO*x*/$FA_{0.3}MA_{0.7}PbI_{3-x}Cl_x$/$PC_{61}BM$/BCP/ Ag/$TeO_2$	18.86	15.12	80.17
	ITO/NiO_X/$FA_{0.3}MA_{0.7}PbI_{3-x}Cl_x$-PEAI/ $PC_{61}BM$ / BCP/Ag	16.07	8.40	52.27
	ITO/NiO_X/$FA_{0.3}MA_{0.7}PbI_{3-x}Cl_x$-PEAI/ $PC_{61}BM$ / BCP/TeO_2/Ag	20.25	16.75	82.72
	ITO/NiO_X/$FA_{0.3}MA_{0.7}PbI_{3-x}Cl_x$-PEAI/ $PC_{61}BM$ / BCP/Ag/TeO_2-with glass reflector	22.51	21.49	95.47
	ITO/NiO*x*/$FA_{0.3}MA_{0.7}PbI_{3-x}Cl_x$-PEAI-PEAI/ $PC_{61}BM$ / BCP/Ag/TeO_2	12.42	10.55	84.94
Yang *et al.,* [31]	ITO/SnO_2/$CH_3NH_3PbI_3$/NiO_X/ITO	8.47	7.10	83.83
Li *et al.,* [32]	ITO/SnO_2/$CH_3NH_3PbI_3$/undoped Spiro-OMeTAD/ sorbitol/PEDOT:PSS/ITO	15.02	13.79	91.81
Liang *et al.,* [33]	ITO/np-SnO_2/ $CH_3NH_3PbI_3$/Spiro-OMeTAD/MoO_X/ Ag/WO_3	15.40	9.70	62.99
Chen *et al.,* [34]	FTO/TiO_2/CsPbIBr$_2$/Spiro-OMeTAD/Ag/TeO_2	8.46	6.40	75.65
Huo *et al.,* [35]	ITO/SnO_2/CsMAFA/CuSCN/MoO_X/ITO/Au	14.80	12.50	84.46
Truong *et al.,* [36]	ITO/SnO_2/$Cs_{0.05}FA_{0.80}MA_{0.15}PbI_{2.75}Br_{0.25}$/HND-$NAr_2$/$MoO_3$/Au/$MoO_3$	10.90	6.80	62.38
	ITO/SnO_2/$Cs_{0.05}FA_{0.80}MA_{0.15}PbI_{2.75}Br_{0.25}$/	12.40	7.80	62.90

	HND-DTP/MoO_3/Au/MoO_3			
	ITO/SnO_2/$Cs_{0.05}FA_{0.80}MA_{0.15}PbI_{2.75}Br_{0.25}$/ HND-Cbz/$MoO_3$/Au/$MoO_3$	11.60	6.10	52.58
	ITO/SnO_2/$Cs_{0.05}FA_{0.80}MA_{0.15}PbI_{2.75}Br_{0.25}$/ Spiro-OMeTAD/$MoO_3$/Au/$MoO_3$	13.0	7.60	58.46
Park *et al.,* [37]	ITO/GO/$CH_3NH_3PbI_3$/C_{60}/PEIE/Ag	12.48	11.45	91.74
Elakshar *et al.,* [38]	ITO/SnO_2/PCBA/$Cs_{0.12}FA_{0.88}PbI_3$/SWCNT	16.30	6.90	42.33
Heo *et al.,* [39]	ITO/PTAA/$Cs_{0.05}(FA_{0.92}MA_{0.08})_{0.95}Pb(I_{0.92}Br_{0.08})_3$/$C_{60}$/BCP/$SnO_2$/ ITO	17.68	16.01	90.55
Jeong *et al.,* [40]	PI@GR(APSIM)/PEDOT:PSS/ $CH_3NH_3PbI_3$/ $CH(NH_2)_2PbI_3$/C_{60}/BCP/PI@GR (TETA)	15.10	13.80	91.39
Najafi *et al.,* [41]	ITO/NiO np + PTAA/$Cs_{0.15}FA_{0.85}Pb(I_{0.92}Br_{0.08})_3$/PCBM/ZnO np/ZnO/ITO	17.20	16.70	97.09
	ITO/NiO np + PTAA/ $Cs_{0.15}FA_{0.85}Pb(I_{0.92}Br_{0.08})_3$/PCBM/Zno np/ZnO/ITO	15.80	14.90	94.30
Zhang *et al.,* [42]	ITO/SnO_2/$Cs_{0.05}FA_{0.85}MA_{0.10}Pb(I_{0.97}Br_{0.03})_3$/Spiro-OMeTAD/MWCNT/ITO/$MgF_2$/IZO/ZnO/CdS/$CuINSe_2$/ Mo/Glass	22.20	10.80	48.65
	ITO/ SnO_2/$Cs_{0.05}FA_{0.85}MA_{0.10}Pb(I_{0.97}Br_{0.03})_3$/Spiro-OMeTAD/SWCNT/ITO//MgF_2/IZO/ZnO/CdS/$CuINSe_2$/Mo/Glass	21.40	16.80	78.50
Fan *et al.,* [43]	ITO/SnO_2/$CH_3NH_3PbI_3$/WS_2 + Spiro-OMeTAD/Ag	19.87	15.48	77.91
Jiang *et al.,* [44]	FTO/MeO-2PACZ/$Rb_{0.05}Cs_{0.05}MA_{0.05}FA_{0.85}Pb(I_{0.95}Br_{0.05})_3$/LiF/$C_{60}$/$SnO_2$/IZO	21.40	20.01	93.50
Zhang *et al.,* [45]	SWCNT/ Cu:NiOx/$Cs_{0.05}FA_{0.80}MA_{0.15}Pb(I_xBr_{1-x})_3$/$SnO_2$/PCBM/SWCNT	18.54	18.22	98.27
Han *et al.,* [46]	FTO/c-TiO_2/SnO_2-Cl/ $(FA_{0.95}Cs_{0.05})PbI_3)_{0.975}(MAPbBr_3)_{0.025}$/Spiro-OMeTAD/$MoO_3$/ITO/Ag/PMMA/$MgF_2$	24.12	21.37	88.60

Albedo factors are one of the important criteria in enhancing the PCE of B-PSCs. The albedo factor was determined as the fraction of incoming solar radiation reflected by each surface [47]. Zhang *et al.,*[45] evaluated the performance of their B-PSCs under various environmental condition with different albedo factors. Figure 2a - 2c shows the angles of light received by B-PSCS that are installed with tilted, horizontal and vertical installing configuration. Figure 2d - 2k shows several common reflection surfaces that contribute to reflected illumination. These surfaces include snow, fiberglass, dry and wet soil, concrete, tile, sand, and grass. Among them, snow exhibited the highest albedo factor with 96% within the wavelength range of 300 to 850 nm, as shown in Figure 3. This followed by fiberglass with 67%, grass 37%, dry soil 34%, sand 28%, wet soil 19%, concreate 18% and tile 12%, respectively.

Structural engineering plays the most crucial role in enhancing the transparency and optical performance of rear electrodes in B-PSCs. Various approaches have been explored, including the use of Fabry–Pérot resonant cavities and Bragg reflectors, which manipulate interference effects to maximize light transmission and reflection [48-55]. Other techniques include the incorporation of photonic crystals and nano-patterned dielectric layers, all of which can be tailored to manage light propagation and minimize parasitic absorption in the rear contact. Pang *et al.,* [21] employed a PEIE/Ag/MoO_X trilayer as the rear electrode in their device architecture. Hanmandlu *et al.,* [22] utilized a BCP/Ag/MoO_3 configuration, while Liang *et al.,* [33] adopted a MoO_X/Ag/MoO_X structure to enhance rear-side transparency and stability.

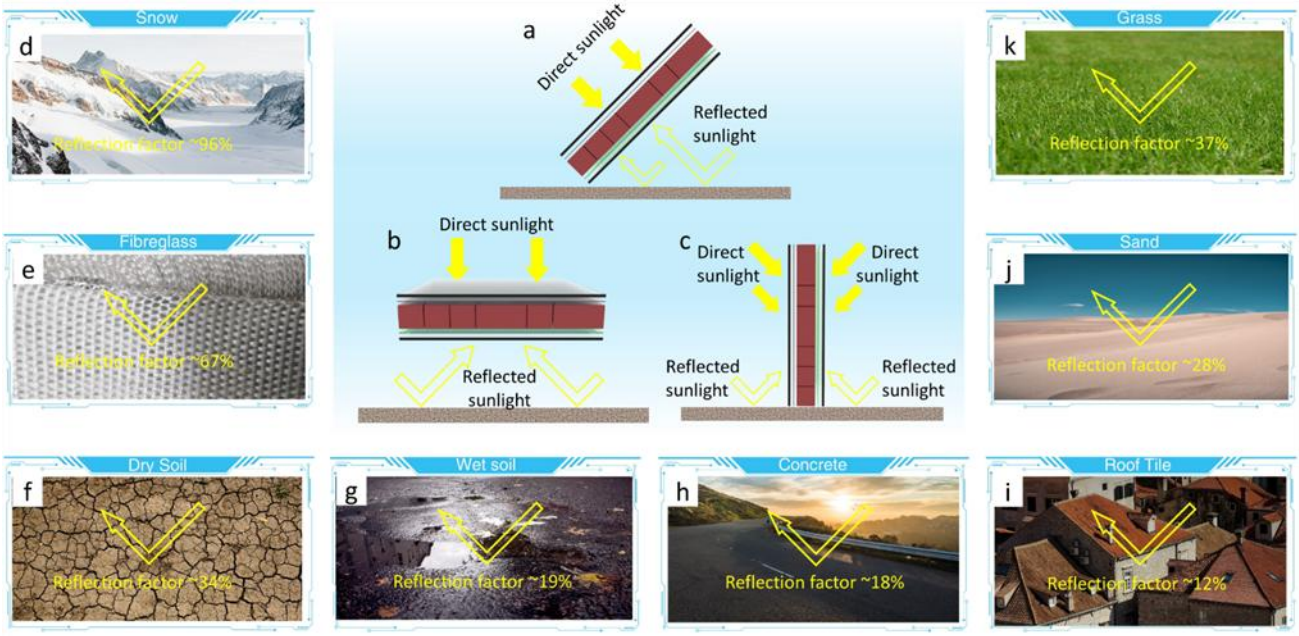

Fig. 2. Angle of light from (a) Titled (b) Horizontal (c) Vertical installing configuration. Reflection surface of (d) Snow (e) Fibreglass (f) Dry soil (g) Wet soil (h) Concreate (i) Roof tile (j) Sand (k) Grass. Credit to photo captured by Erol Ahmed, Mike Erskine, Jens Freudenau, Joshua Sortino, Maxim Berg, Colin Lloyd on Uplash. Reproduced under CC-BY license. Copyright 2024 Springer Nature [45]

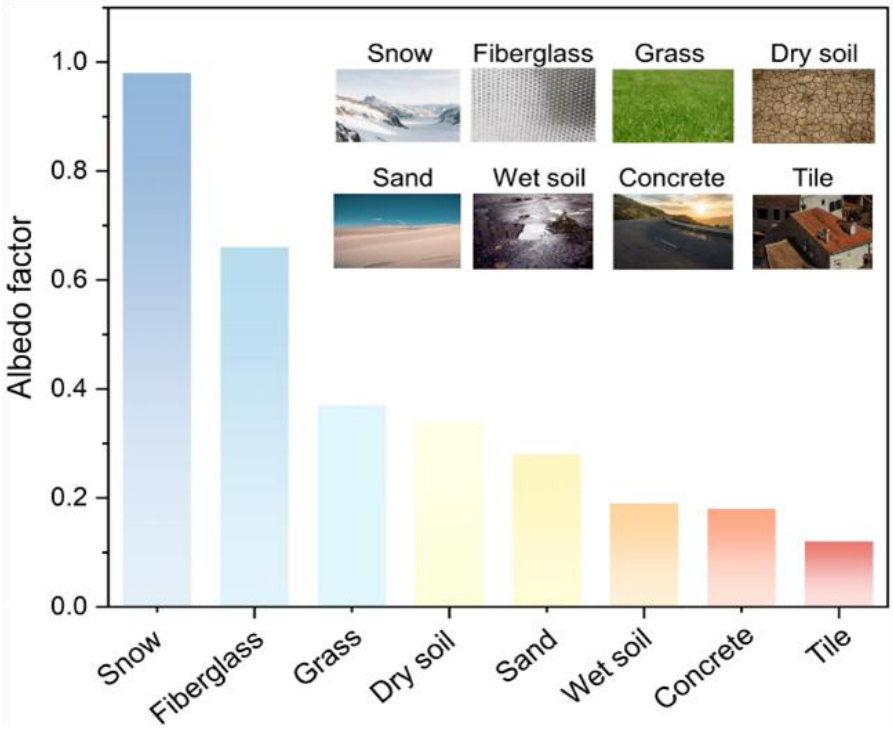

Fig. 3. Albedo factor of eight common ground. Reproduced under CC-BY license. Copyright 2024 Springer Nature [45]

Figure 4 presents the structural and morphological characteristics of a B-PSCs incorporating a BCP/Ag/MoO_3 rear electrode. The schematic in Figure 4a outlines the overall device architecture, highlighting its light penetrate from direct illumination and reflected light from albedo effect. A cross-sectional SEM image (Figure 4b) reveals the layered configuration of the cell, confirming the integration of the BCP/Ag/MoO_3 stack with its film shows highest transparency. Figure 4c and 4d

show SEM surface images of BCP/Ag films with varying BCP/Ag silver thicknesses, demonstrating changes in film uniformity and morphology; inset photographs further illustrate the corresponding optical transparency of each film on glass substrates. Lastly, Figure 4e displays the fabricated semitransparent device, visually confirming the transparency and structural integrity of the electrode stack, which is critical for enabling rear-side light harvesting in bifacial configurations. This configuration resulting PCE of 13.49% from front-side and 9.61% from rear-side resulting BF with 71.23% [22].

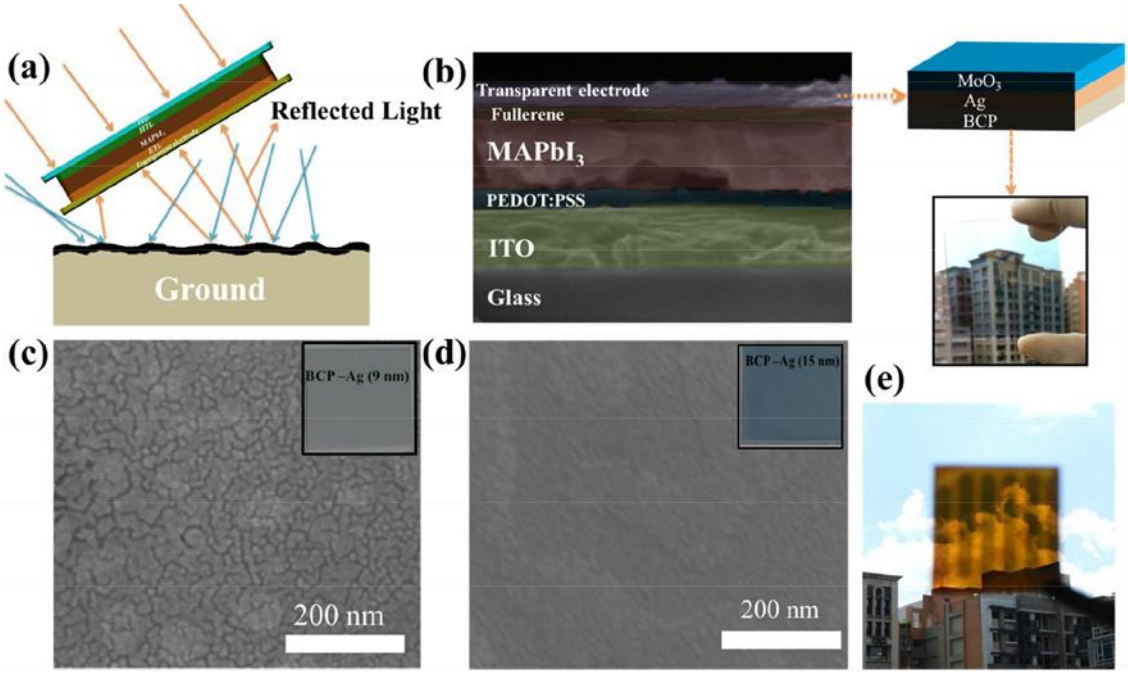

Fig. 4. Structural and morphological characteristics of a B-PSCs incorporating a BCP/Ag/MoO_3 rear electrode (a) Illustration of the device architecture (b) Cross-sectional SEM for whole device and film image of BCP/Ag/MoO_3 layer (c) and (d) SEM surface images of BCP 8 nm/Ag 9 nm and BCP 8 nm/Ag 15 nm, with insets displaying image of films deposited on glass substrates (e) Image of a semitransparent PSCs incorporating the BCP/Ag/MoO_3 electrode structure. Reproduced from Ref. [22] Copyright 2017 American Chemical Society

4. Challenges and Future Directions in B-PSCs

4.1 Challenges

4.1.1 Rear electrode transparency

Achieving a high degree of transparency in the rear electrode is essential for efficient bifacial light harvesting; however, it often comes at the expense of electrical conductivity. Materials like ITO and FTO offer good transparency but suffer from brittleness and limited scalability. Meanwhile, ultrathin metal films and transparent conductive polymers provide flexible alternatives but typically exhibit higher sheet resistance and reduced durability. Balancing optical transmittance, electrical performance, and long-term reliability remains a significant challenge.

4.1.2 Stability

Material stability is a critical concern in B-PSC. Although perovskite materials exhibit excellent optoelectronic properties, they are inherently vulnerable to environmental stressors. Moisture, oxygen, UV radiation, and thermal cycling can degrade the perovskite layer and adjacent interfaces,

leading to phase decomposition and ion migration. In bifacial configurations, where both sides are exposed to the environment, the risk of degradation is even more pronounced. This necessitates the development of robust material compositions and interface engineering strategies that enhance intrinsic stability without compromising device performance.

4.1.3 Encapsulation of dual-sided exposure

Conventional encapsulation techniques, designed primarily for monofacial cells, are inadequate for bifacial architectures. Bifacial devices require symmetrical, transparent encapsulation on both front and rear sides to allow unhindered light entry while ensuring mechanical protection and environmental sealing. Developing encapsulants that combine high optical clarity, low water vapor transmission rates, UV resistance, and mechanical flexibility is particularly challenging. Moreover, ensuring compatibility between the encapsulant and various device layers without introducing interfacial degradation pathways is a critical requirement

4.1.4 Process scalability for large-area devices

Scaling B-PSC from laboratory-scale prototypes to industrially viable modules are hindered by challenges in maintaining uniformity over large areas. Achieving defect-free perovskite films with consistent thickness, grain size, and crystallinity is difficult at scale, particularly with solution-based deposition techniques. Additionally, large-area coating of transparent electrodes with low resistivity and high durability remains an unresolved issue. These fabrication inconsistencies lead to performance losses and reduced yield, limiting the commercial potential of bifacial perovskite technology.

4.2 Future Directions

4.2.1 Advanced light management structures

Optimizing light management is key to maximizing the bifacial gain in perovskite solar cells. Integrating nanophotonic structures, such as photonic crystals, diffraction gratings, or plasmonic nanoparticles, can manipulate light paths to enhance absorption in the active layer from both the front and rear sides. Additionally, the use of textured substrates or reflective coatings can increase albedo utilization, particularly in diffuse light environments. These advanced designs not only improve photocurrent generation but also contribute to angular insensitivity and energy yield enhancement under real-world conditions.

4.2.2 Development of durable transparent electrodes

Future research should focus on developing rear electrodes that simultaneously offer high transparency, low sheet resistance, and robust environmental stability. Emerging materials such as doped metal oxides (e.g., AZO, GZO), graphene composites, and silver nanowire networks are promising candidates. These alternatives must be optimized for compatibility with perovskite layers and scalable fabrication techniques. Multilayer hybrid electrodes that combine metallic and dielectric components may also provide a tunable platform to meet performance and durability criteria for bifacial operation.

4.2.3 Development of advanced perovskite materials and stabilization techniques

The future success of B-PSCs heavily depends on the development of perovskite materials with improved intrinsic stability and higher photoelectric conversion efficiency. Research is increasingly focused on compositional engineering, such as the incorporation of mixed cations (e.g., FA^+, Cs^+) and halides (e.g., I^-/Br^-) to form more stable and defect-tolerant perovskite phases. Furthermore, the application of molecular cross-linking techniques has shown significant promise in enhancing the performance of solar cell [14,56,57]. Other promising approaches include surface passivation using 2D perovskite layers, incorporation of polymeric interlayers, and solvent engineering during film formation to achieve uniform crystal growth [58]. These combined strategies aim to produce high-efficiency, moisture- and UV-resistant films suitable for long-term outdoor bifacial operation.

4.2.4 Field testing and modeling under real conditions

To bridge the gap between lab-scale efficiency and practical performance, extensive field testing under varied climatic and albedo conditions is essential. Such studies should evaluate long-term stability, bifacial gain, and energy yield in diverse environments. Moreover, integrating real-time monitoring data with machine learning models can aid in predictive performance modeling, enabling the design of adaptive systems tailored to specific geographies [59]. These insights will guide material selection, module design, and system optimization for widespread deployment.

5. Conclusions

B-PSCs represent a promising avenue for next-generation photovoltaic technologies, offering the potential for higher energy yield through dual-sided light harvesting. Over the past decade, significant progress has been made in material design, device architecture, and optical management strategies, enabling notable gains in efficiency and bifacial performance. However, challenges such as environmental stability, scalable fabrication, and reliable encapsulation remain critical barriers to commercial deployment. Continued research into robust materials, advanced transparent electrodes, and real-world performance modeling will be essential to unlock the full potential of bifacial perovskite technology in practical energy applications.

Acknowledgement
Author acknowledges the support provided by the Geran Galakan Penyelidik Muda (GGPM), grant number GGPM-2023-048, funded by the Universiti Kebangsaan Malaysia (UKM), Malaysia.

Conflict of Interest Statement
The author declares that there are no conflicts of interest related to the publication of this manuscript.

Author Contributions Statement
S.S. was responsible for the conceptualization, validation, formal analysis, investigation, resources, visualization, original draft preparation, review and editing of the manuscript, and project administration.

Data Availability Statement

No datasets were generated or analysed during the current study.

Ethics Statement

This study did not involve human participants, animals, or sensitive data, and therefore did not require ethical approval.

References

[1] Sinha, Numeshwar Kumar, Dhriti Sundar Ghosh, and Ayush Khare. "Highly efficient, low-cost, lead-free bifacial perovskite solar cells: A designing strategy through simulation." *Next Materials* 4 (2024): 100219. https://doi.org/10.1016/j.nxmate.2024.100219

[2] Rabhi, Selma, Tarak Hidouri, Souraya Goumri-Said, Hussain J. Alathlawi, Ghayah M. Alsulaim, and Mir Waqas Alam. "Bifacial perovskite solar cells with> 21% efficiency: Computational insights into novel HTLs materials and architectures." *Solar Energy* 284 (2024): 113083. https://doi.org/10.1016/j.solener.2024.113083

[3] Shafian, Shafidah. "Semitransparent and Colorful Solar Cell for Architectural Application." *Future Energy and Environment Letters* 2, no. 1 (2025): 13-32. https://doi.org/10.37934/feel.2.1.1332

[4] Tina, Giuseppe Marco, Fausto Bontempo Scavo, Leonardo Merlo, and Fabrizio Bizzarri. "Comparative analysis of monofacial and bifacial photovoltaic modules for floating power plants." *Applied Energy* 281 (2021): 116084. https://doi.org/10.1016/j.apenergy.2020.116084

[5] Riaz, Muhammad Hussnain, Hassan Imran, Rehan Younas, and Nauman Zafar Butt. "The optimization of vertical bifacial photovoltaic farms for efficient agrivoltaic systems." *Solar Energy* 230 (2021): 1004-1012. https://doi.org/10.1016/j.solener.2021.10.051

[6] Gupta, Vaibhav, Prasun Kumar, and Ranbir Singh. "Unveiling the potential of bifacial photovoltaics in harvesting indoor light energy: a comprehensive review." *Solar Energy* 276 (2024): 112660. https://doi.org/10.1016/j.solener.2024.112660

[7] Singh, Ranbir, Prasun Kumar, Pankaj Kumar, Sumit Chaudhary, Zhipeng Kan, Vikrant Sharma, and Satinder K. Sharma. "Indoor bifacial perovskite photovoltaics: efficient energy harvesting from artificial light sources." *Solar Energy* 264 (2023): 112061. https://doi.org/10.1016/j.solener.2023.112061

[8] Chand, Lal, Prasun Kumar, Rahul Tiwari, Milon Kundar, Suman Kalyan Pal, Vibha Saxena, Ranbir Singh, and Surya Prakash Singh. "Impact of tailoring BTBT-based hole-transporting materials on perovskite photovoltaics under indoor illumination." *Sustainable Energy & Fuels* 8, no. 23 (2024): 5458-5466. https://doi.org/10.1039/D4SE00998C

[9] Singh, Ranbir, Vivek Kumar Shukla, Mritunjaya Parashar, Vikrant Sharma, and Satinder Kumar Sharma. "Highly efficient quasi-cubic structured perovskite for harvesting energy from artificial indoor LED light source." *Solar Energy* 245 (2022): 332-339. https://doi.org/10.1016/j.solener.2022.09.015

[10] Sinha, Numeshwar Kumar, Dhriti Sundar Ghosh, and Ayush Khare. "A comprehensive guide to bifacial perovskite solar cells: simulation and optimization." *Advanced Theory and Simulations* 7, no. 1 (2024): 2300633. https://doi.org/10.1002/adts.202300633

[11] Alathlawi, Hussain J., Selma Rabhi, Tarak Hidouri, Hind Adawi, Fadiyah A. Makin, and Amani A. Alsam. "Role of Ag Nanowires: MXenes in Optimizing Flexible, Semitransparent Bifacial Inverted Perovskite Solar Cells for Building-Integrated Photovoltaics: A SCAPS-1D Modeling Approach." *Advanced Theory and Simulations* 8, no. 3 (2025): 2401004. https://doi.org/10.1002/adts.202401004

[12] Qi, Shuwen, Chenghao Ge, Peng Wang, Bin Wu, Yuping Zhao, Rongjun Zhao, Shafidah Shafian, Yong Hua, and Lin Xie. "Improving Perovskite Solar Cell Performance and Stability via Thermal Imprinting-Assisted Ion Exchange Passivation." *ACS Applied Materials & Interfaces* 16, no. 38 (2024): 51037-51045. https://doi.org/10.1021/acsami.4c08538

[13] Wang, Peng, Shafidah Shafian, Feng Qiu, Xiao Zhang, Yuping Zhao, Bin Wu, Kyungkon Kim, Yong Hua, and Lin Xie. "Improving redox reactions of Spiro-OMeTAD via p-type molecular scaffold to reduce energy loss at Ag-electrode in perovskite solar cells." *Journal of Energy Chemistry* 102 (2025): 151-160. https://doi.org/10.1016/j.jechem.2024.10.027

[14] Zhang, Xiao, Linqing Wang, Shafidah Shafian, Peng Wang, Yuping Zhao, Pengcheng Wang, Bin Wu et al. "Crosslinking-Driven Chemical Homogeneity Enhances Performance of Pre-Seeded Perovskite Solar Cells." *Small* 21, no. 6 (2025): 2408362. https://doi.org/10.1002/smll.202408362

[15] Lee, Sojeong, Young Seon Yoon, Shafidah Shafian, Jin Young Kim, and Kyungkon Kim. "Sequential Co-Deposition of Perovskite Film: An Effective Way of Tailoring Bandgap in All Vacuum Processed Perovskite Solar Cells." *Small Methods* (2025): 2500104. https://doi.org/10.1002/smtd.202500104

[16] Shin, Solbi, Shafidah Shafian, Ka Yeon Ryu, Young-Kyo Jeon, Won-Suk Kim, and Kyungkon Kim. "Solution-Processed TiO_2 Nanoparticles Functionalized with Catechol Derivatives as Electron Transporting Layer Materials for Organic Photovoltaics." *Advanced Materials Interfaces* 9, no. 14 (2022): 2200118. https://doi.org/10.1002/admi.202200118

[17] Ryu, Ka Yeon, Shafidah Shafian, Jongchan Shin, Yu Jin Lee, Minjae Lee, and Kyungkon Kim. "Linear polyurethane ionenes for stable interlayer of organic photovoltaics." *Journal of Power Sources* 542 (2022): 231772. https://doi.org/10.1016/j.jpowsour.2022.231772

[18] Shafian, Shafidah, Heewon Hwang, and Kyungkon Kim. "Near infrared organic photodetector utilizing a double electron blocking layer." *Optics Express* 24, no. 22 (2016): 25308-25316. https://doi.org/10.1364/OE.24.025308

[19] Fu, Fan, Thomas Feurer, Timo Jäger, Enrico Avancini, Benjamin Bissig, Songhak Yoon, Stephan Buecheler, and Ayodhya N. Tiwari. "Low-temperature-processed efficient semi-transparent planar perovskite solar cells for bifacial and tandem applications." *Nature communications* 6, no. 1 (2015): 8932. https://doi.org/10.1038/ncomms9932

[20] Xiao, Yaoming, Gaoyi Han, Jihuai Wu, and Jeng-Yu Lin. "Efficient bifacial perovskite solar cell based on a highly transparent poly (3, 4-ethylenedioxythiophene) as the p-type hole-transporting material." *Journal of Power Sources* 306 (2016): 171-177. https://doi.org/10.1016/j.jpowsour.2015.12.003

[21] Pang, Shangzheng, Dazheng Chen, Chunfu Zhang, Jingjing Chang, Zhenhua Lin, Haifeng Yang, Xu Sun, Jiajie Mo, He Xi, Genquan Han, Jincheng Zhang and Yue Hao "Efficient bifacial semitransparent perovskite solar cells with silver thin film electrode." *Solar Energy Materials and Solar Cells* 170 (2017): 278-286. https://doi.org/10.1016/j.solmat.2017.05.071

[22] Hanmandlu, Chintam, Chien-Yu Chen, Karunakara Moorthy Boopathi, Hao-Wu Lin, Chao-Sung Lai, and Chih-Wei Chu. "Bifacial perovskite solar cells featuring semitransparent electrodes." *ACS applied materials & interfaces* 9, no. 38 (2017): 32635-32642. https://doi.org/10.1021/acsami.7b06607

[23] Fan, Lin, Yuelong Li, Xin Yao, Yi Ding, Shanzhen Zhao, Biao Shi, Changchun Wei *et al.,* "Delayed annealing treatment for high-quality CuSCN: Exploring its impact on bifacial semitransparent n-i-p planar perovskite solar cells." *ACS Applied Energy Materials* 1, no. 4 (2018): 1575-1584. https://doi.org/10.1021/acsaem.8b00001

[24] Martínez-Denegri, Guillermo, Silvia Colodrero, Mariia Kramarenko, and Jordi Martorell. "All-nanoparticle SnO_2/TiO_2 electron-transporting layers processed at low temperature for efficient thin-film perovskite solar cells." *ACS Applied Energy Materials* 1, no. 10 (2018): 5548-5556. https://doi.org/10.1021/acsaem.8b01118

[25] DeLuca, Giovanni, Askhat N. Jumabekov, Yinghong Hu, Alexandr N. Simonov, Jianfeng Lu, Boer Tan, Gede W. P. Adhyaksa, Erik C. Garnett, Elsa Reichmanis, Anthony S. R. Chesman, and Udo Bach. "Transparent quasi-interdigitated electrodes for semitransparent perovskite back-contact solar cells." *ACS Applied Energy Materials* 1, no. 9 (2018): 4473–4478. https://doi.org/10.1021/acsaem.8b01140

[26] Pang, Shangzheng, Xueyi Li, Hang Dong, Dazheng Chen, Weidong Zhu, Jingjing Chang, Zhenhua Lin, He Xi, Jincheng Zhang, Chunfu Zhang, and Yue Hao. "Efficient bifacial semitransparent perovskite solar cells using Ag/V_2O_5 as transparent anodes." *ACS Applied Materials & Interfaces* 10, no. 15 (2018): 12731–12739. https://doi.org/10.1021/acsami.8b01611

[27] Li, Yanan, Jialong Duan, Yuanyuan Zhao, and Qunwei Tang. "All-inorganic bifacial $CsPbBr_3$ perovskite solar cells with a 98.5%-bifacial factor." *Chemical communications* 54, no. 59 (2018): 8237-8240. https://doi.org/10.1039/C8CC04271C

[28] Lee, Kun-Mu, Kai-Shiang Chen, Jia-Ren Wu, Yan-Duo Lin, Sheng-Min Yu, and Sheng Hsiung Chang. "Highly efficient and stable semi-transparent perovskite solar modules with a trilayer anode electrode." *Nanoscale* 10, no. 37 (2018): 17699-17704. https://doi.org/10.1039/C8NR06095A

[29] Chiang, Yu-Hsien, Chieh-Chung Peng, Yu-Hung Chen, Yung-Liang Tung, Song-Yeu Tsai, and Peter Chen. "The utilization of IZO transparent conductive oxide for tandem and substrate type perovskite solar cells." *Journal of Physics D: Applied Physics* 51, no. 42 (2018): 424002. https://doi.org/10.1088/1361-6463/aad71c

[30] Chen, Dazheng, Shangzheng Pang, Long Zhou, Xueyi Li, Aixue Su, Weidong Zhu, Jingjing Chang, Jincheng Zhang, Chunfu Zhang, and Yue Hao. "An efficient TeO 2/Ag transparent top electrode for 20%-efficiency bifacial perovskite solar cells with a bifaciality factor exceeding 80%." *Journal of Materials Chemistry A* 7, no. 25 (2019): 15156-15163. https://doi.org/10.1039/C9TA02389E

[31] Yang, Yujing, Yue Zhu, Xiaoxiao Wang, Qi Song, Chao Ji, Huimin Zhang, Zhiqun He, and Chunjun Liang. "Laminating Fabrication of Bifacial Organic-Inorganic Perovskite Solar Cells." *International Journal of Photoenergy* 2020, no. 1 (2020): 5039192. https://doi.org/10.1155/2020/5039192

[32] Li, Tianyang, Wiley A. Dunlap-Shohl, and David B. Mitzi. "Bifacial perovskite solar cells via a rapid lamination process." *ACS Applied Energy Materials* 3, no. 10 (2020): 9493-9497. https://doi.org/10.1021/acsaem.0c00756

[33] Liang, Fengxia, Zhiqin Ying, Yi Lin, Bao Tu, Zheng Zhang, Yudong Zhu, Hui Pan, Haifeng Li, Linbao Luo, Oleg Ageev, and Zhubing He. "High-Performance Semitransparent and Bifacial Perovskite Solar Cells with MoOx/Ag/WOx as the Rear Transparent Electrode." *Advanced Materials Interfaces* 7, no. 20 (2020): 2000591. https://doi.org/10.1002/admi.202000591

[34] Chen, Dazheng, Gang Fan, Weidong Zhu, Haifeng Yang, He Xi, Fengqing He, Zhenhua Lin, Jincheng Zhang, Chunfu Zhang, and Yue Hao. "Highly efficient bifacial $CsPbIBr_2$ solar cells with a TeO_2/Ag transparent electrode and unsymmetrical carrier transport behavior." *Dalton Transactions* 49, no. 18 (2020): 6012–6019. https://doi.org/10.1039/D0DT00407C

[35] Hou, Shixin, Biao Shi, Pengyang Wang, Yucheng Li, Jie Zhang, Peirun Chen, Bingbing Chen, Fuhua Hou, Qian Huang, and Yi Ding. "Highly efficient bifacial semitransparent perovskite solar cells based on molecular doping of CuSCN hole transport layer." *Chinese Physics B* 29, no. 7 (2020): 078801. https://doi.org/10.1088/1674-1056/ab99ae

[36] Truong, Minh Anh, Hayoon Lee, Ai Shimazaki, Ryota Mishima, Masashi Hino, Kenji Yamamoto, Kento Otsuka, Taketo Handa, Yoshihiko Kanemitsu, Richard Murdey, and Atsushi Wakamiya. "Near-ultraviolet transparent organic hole-transporting materials containing partially oxygen-bridged triphenylamine skeletons for efficient perovskite solar cells." *ACS Applied Energy Materials* 4, no. 2 (2021): 1484–1495. https://doi.org/10.1021/acsaem.0c02677

[37] Park, Min-Ah, Sae Jin Sung, You Jin Ahn, Inhwa Hong, Ik Jae Park, Chong Rae Park, and Jin Young Kim. "Bifunctional graphene oxide hole-transporting and barrier layers for transparent bifacial flexible perovskite solar cells." *ACS Applied Energy Materials* 4, no. 9 (2021): 8824–8831. https://doi.org/10.1021/acsaem.1c00928

[38] Elakshar, Aly, Sergey Tsarev, Pramod Mulbagal Rajanna, Marina Tepliakova, Lyubov Frolova, Yuriy G. Gladush, Sergey M. Aldoshin, Pavel A. Troshin, and Albert G. Nasibulin. "Surface passivation for efficient bifacial HTL-free perovskite solar cells with SWCNT top electrodes." *ACS Applied Energy Materials* 4, no. 12 (2021): 13395–13400. https://doi.org/10.1021/acsaem.1c02134

[39] Heo, Jihyeon, Incheol Jung, Hyunwoo Park, Ju Hwan Han, Hyeonwoo Kim, Hansol Park, Jin-Seong Park, Hyeongtag Jeon, Kyu-Tae Lee, and Hui Joon Park. "Highly efficient bifacial color-tunable perovskite solar cells." *Advanced Optical Materials* 10, no. 2 (2022): 2101696. https://doi.org/10.1002/adom.202101696

[40] Jeong, Gyujeong, Donghwan Koo, Jeong-Hyun Woo, Yunseong Choi, Eunbin Son, Fuzhi Huang, Ju-Young Kim, and Hyesung Park. "Highly efficient self-encapsulated flexible semitransparent perovskite solar cells via bifacial cation exchange." *ACS Applied Materials & Interfaces* 14, no. 29 (2022): 33297–33305. https://doi.org/10.1021/acsami.2c08023

[41] Najafi, Mehrdad, Mirjam Theelen, Henri Fledderus, Dong Zhang, Valerio Zardetto, Bas van Aken, and Sjoerd Veenstra. "Light-Soak Stable Semitransparent and Bifacial Perovskite Solar Cells for Single-Junction and Tandem Architectures." *Solar RRL* 6, no. 4 (2022): 2100621. https://doi.org/10.1002/solr.202100621

[42] Zhang, Chunyang, Min Chen, Fan Fu, Hongwei Zhu, Thomas Feurer, Wenming Tian, Chao Zhu, Ke Zhou, Shengye Jin, Shaik Mohammed Zakeeruddin, Ayodhya N. Tiwari, Nitin P. Padture, Michael Grätzel, and Yantao Shi. "CNT-based bifacial perovskite solar cells toward highly efficient 4-terminal tandem photovoltaics." *Energy & Environmental Science* 15, no. 4 (2022): 1536–1544. https://doi.org/10.1039/D1EE04008A

[43] Fan, Lin, Wanhong Lü, Wanting Hu, Donglai Han, Shuo Yang, Dandan Wang, Zhihong Mai et al. "Enhanced photovoltaic output of bifacial perovskite solar cells via tailoring photoelectric balance in rear window layers with 1T-WS 2 nanosheet engineering." *Materials Chemistry Frontiers* 6, no. 15 (2022): 2061-2071. https://doi.org/10.1039/D2QM00366J

[44] Jiang, Qi, Zhaoning Song, Rosemary C. Bramante, Paul F. Ndione, Robert Tirawat, Joseph J. Berry, Yanfa Yan, and Kai Zhu. "Highly efficient bifacial single-junction perovskite solar cells." *Joule* 7, no. 7 (2023): 1543-1555. https://doi.org/10.1016/j.joule.2023.06.001

[45] Zhang, Jing, Xian-Gang Hu, Kangyu Ji, Songru Zhao, Dongtao Liu, Bowei Li, Peng-Xiang Hou, Chang Liu, Lirong Liu, Samuel D. Stranks, Hui-Ming Cheng, S. Ravi P. Silva, and Wei Zhang. "High-performance bifacial perovskite solar cells enabled by single-walled carbon nanotubes." *Nature Communications* 15, no. 1 (2024): 2245. https://doi.org/10.1038/s41467-024-46620-1

[46] Han, Yaliang, Xiaopeng Feng, Yijin Wei, Lin Han, Bingqian Zhang, Qichao Meng, Boyang Lu, Changcheng Cui, Hao Wei, Yimeng Li, Zucheng Wu, Rongxiu Liu, Shengren Xia, Xiao Wang, Qingfu Wang, Lan Cao, Zhipeng Shao, Shuping Pang, and Guanglei Cui. "The multifunctional antireflection layer of a bifacial perovskite $((FA_{0.95}Cs_{0.05})PbI_3)_{0.975}(MAPbBr_3)_{0.025})$ solar cell enhances its bifaciality, stability, and environmental adaptability." *ACS Materials Letters* 7, no. 3 (2025): 1077–1084. https://doi.org/10.1021/acsmaterialslett.5c00115

[47] Tonita, Erin M., Christopher E. Valdivia, Annie CJ Russell, Michael Martinez-Szewczyk, Mariana I. Bertoni, and Karin Hinzer. "Quantifying spectral albedo effects on bifacial photovoltaic module measurements and system model predictions." *Progress in Photovoltaics: Research and Applications* 32, no. 7 (2024): 468-480. https://doi.org/10.1002/pip.3789

[48] Kim, Bo Youn, Shafidah Shafian, and Kyungkon Kim. "High-Performance Semitransparent Color Organic Photodiodes Enabled by Integrating Fabry–Perot and Solution-Processed Distributed Bragg Reflectors." *Advanced Materials Interfaces* 10, no. 31 (2023): 2300421. https://doi.org/10.1002/admi.202300421

[49] Salehin, Fitri Norizatie Mohd, Puvaneswaran Chelvanathan, Adamu Ahmed Goje, Norasikin Ahmad Ludin, Mohd Adib Ibrahim, and Shafidah Shafian. "Design of blue, green and red colorful semitransparent films using Ag/SnO_2/Ag color filter for integrated into solar cells." *Results in Physics* 70 (2025): 108172. https://doi.org/10.1016/j.rinp.2025.108172

[50] Park, Suhyeon, Shafidah Shafian, Juhwan Lee, Seungyun Jo, Seungbae Jeon, Seungjae Lee, Ding Shangxian, Hyungju Ahn, Kyungkon Kim, and Du Yeol Ryu. "High-efficiency structural coloration enabled by defect-free block copolymer self-assembly for a solar cell distributed Bragg reflector." *Advanced Optical Materials* 11, no. 24 (2023): 2301357. https://doi.org/10.1002/adom.202301357

[51] Shafian, Shafidah, and Kyungkon Kim. "Panchromatically responsive organic photodiodes utilizing a noninvasive narrowband color electrode." *ACS Applied Materials & Interfaces* 12, no. 47 (2020): 53012–53020. https://doi.org/10.1021/acsami.0c17183

[52] Shafian, Shafidah, Ga Eun Lee, Hyeonggeun Yu, Jeung-hyun Jeong, and Kyungkon Kim. "High-efficiency vivid color CIGS solar cell employing nondestructive structural coloration." *Solar RRL* 6, no. 4 (2022): 2100965. https://doi.org/10.1002/solr.202100965

[53] You, Young-Jun, Muhammad Ahsan Saeed, Shafidah Shafian, Jisoo Kim, Sang Hyeon Kim, Sung Hyeon Kim, Kyungkon Kim, and Jae Won Shim. "Energy recycling under ambient illumination for internet-of-things using metal/oxide/metal-based colorful organic photovoltaics." *Nanotechnology* 32, no. 46 (2021): 465401. https://doi.org/10.1088/1361-6528/ac13e7

[54] Shafian, Shafidah, Jieun Son, Youngji Kim, Jerome K. Hyun, and Kyungkon Kim. "Active-material-independent color-tunable semitransparent organic solar cells." *ACS Applied Materials & Interfaces* 11, no. 21 (2019): 18887–18895 https://doi.org/10.1021/acsami.9b03254

[55] Kim, Youngji, Jieun Son, Shafidah Shafian, Kyungkon Kim, and Jerome K. Hyun. "Semitransparent blue, green, and red organic solar cells using color filtering electrodes." *Advanced Optical Materials* 6, no. 13 (2018): 1800051. https://doi.org/10.1002/adom.201800051

[56] Kim, Hyunkyoung, Yuchan Heo, Yeji Na, Shafidah Shafian, BongSoo Kim, and Kyungkon Kim. "Cross-linking-integrated sequential deposition: A method for efficient and reproducible bulk heterojunctions in organic solar cells." *ACS Applied Materials & Interfaces* 16, no. 41 (2024): 55873–55880. https://doi.org/10.1021/acsami.4c13237

[57] Kim, Hyunkyoung, Ye-Jin Kong, Won-Suk Kim, Shafidah Shafian, and Kyungkon Kim. "Enhancing reproducibility in organic solar cell fabrication via static sequential deposition with cross-linked polymer donor and nonfullerene acceptor." *ACS Applied Polymer Materials* 6, no. 10 (2024): 5814–5821. https://doi.org/10.1021/acsapm.4c00477

[58] Hong, Minjeong, Jiyae Youn, Ka Yeon Ryu, Shafidah Shafian, and Kyungkon Kim. "Improving the stability of non-fullerene-based organic photovoltaics through sequential deposition and utilization of a quasi-orthogonal solvent." *ACS Applied Materials & Interfaces* 15, no. 16 (2023): 20151–20158. https://doi.org/10.1021/acsami.3c02071

[59] Shafian, Shafidah, Fitri Norizatie Mohd Salehin, Sojeong Lee, Azlan Ismail, Shuhaida Mohamed Shuhidan, Lin Xie, and Kyungkon Kim. "Development of organic semiconductor materials for organic solar cells via the integration of computational quantum chemistry and AI-powered machine learning." *ACS Applied Energy Materials* 8, no. 2 (2025): 699-722. https://doi.org/10.1021/acsaem.4c02937